



Unprecedented rearrangement during the formation of P–P homoatomic N-phosphino formamidine complexes

Thanh D. Le^a, Damien Arquier^a, Karinne Miqueu^b, Jean-Marc Sotiropoulos^b, Yannick Coppel^a, Stéphanie Bastin^a, Alain Igau^{a,*}

^aLaboratoire de Chimie de Coordination, CNRS, 205 Route de Narbonne, 31077 Toulouse, Cedex 4, France

^bUniversité de Pau et des Pays de l'Adour, UMR CNRS 5254, IPREM, 2 avenue du Président Angot 64053 Pau cedex 09, France

ARTICLE INFO

Article history:

Received 5 September 2008

Received in revised form 15 October 2008

Accepted 16 October 2008

Available online 25 October 2008

Keywords:

Phosphorus

Formamidine

Donor–acceptor systems

NMR spectroscopy

DFT theoretical calculations

ABSTRACT

A variety of homoatomic P–P donor–acceptor homoleptic ($R = R'$) and heteroleptic ($R \neq R'$) N-phosphino formamidine complexes $[iPr_2N-C(H)=N-PR_2-PR'_2]Cl$ were synthesized from the addition of N-phosphino formamidine (phosfam) donor reagent $iPr_2N-C(H)=N-PR_2$ on halogenophosphane compounds R'_2P-Cl which are synthetic sources for the corresponding phosphonium derivatives R'_2P^+ . We have demonstrated that the dynamic equilibrium observed between the different species is shifted either completely to the side of the free species or to the side of the donor–acceptor adduct $[iPr_2N-C(H)=N-PPh_2-PPh_2]Cl$ by changing the solvent or by varying the temperature. Activation parameters of $\Delta S^\ddagger = (-130 \pm 7.2) J mol^{-1} K^{-1}$, $\Delta H^\ddagger = (8.4 \pm 0.6) kJ mol^{-1}$ and $\Delta G^\ddagger (298.15 K) = (53.6 \pm 2.3) kJ mol^{-1}$ were determined by an Eyring analysis over the temperature range of 193–293 K. The negative entropy of activation is consistent with an associative pathway and the low value of ΔH^\ddagger suggests that the energy barrier for this reaction is entropically controlled. Phosphine–phosphonium adducts is the most appropriate term to describe the dynamic process observed at variable temperature for complexes $[iPr_2N-C(H)=N-PR_2 \rightarrow PR'_2]^+$, but the ^{31}P NMR chemical shift and the calculated electronic charges are more in favor of a phosphinophosphonium Lewis drawing $[iPr_2N-C(H)=N-PR_2-PR'_2]^+$. Formation of the homoatomic P–P heteroleptic formamidine complexes $[iPr_2N-C(H)=N-PR_2-PR'_2]Cl$ ($R = Ph$, $R' = Et$, iPr) results in the formal insertion of the phosphino group of the corresponding alkyl chlorophosphanes R'_2P-Cl into the N–P bond of the starting phosfam ligand $iPr_2N-C(H)=N-PR_2$. Computed data are in agreement with the transient formation of a heteroatomic N–P intermediate $[iPr_2N-C(H)=N(PR_2)PR'_2]Cl$, which then rearranges to the more thermodynamically favored homoatomic P–P compound $[iPr_2N-C(H)=N-PR_2-PR'_2]Cl$.

© 2008 Elsevier B.V. All rights reserved.

1. Introduction

In *p*-block coordination chemistry, electron-rich and electron-deficient centers form donor–acceptor bonds; these electron pair donor (EPD)–electron pair acceptor (EPA) systems have been known for a long time [1]. EPD/EPA complexes with phosphonium ions R'_2P^+ as Lewis acceptors have been largely reviewed [2]. The quantitative nature of the reactions and the structural simplicity of the complexes contribute to the new development of *p*-block coordination chemistry [3]. Homoatomic P–P [4] and heteroatomic N–P [5] coordination compounds introduce novel bonding possibilities and new synthetic opportunities. Electrophilic phosphonium acceptors R'_2P^+ form adducts with neutral donor bases, as exemplified by the formation of phosphane **I** [2b,4], amine **II** [5c,d,e], pyridine **III** [5a,c,h], and cyclic amidinephosphonium

compounds **IV** [5b,e,g] (Fig. 1). In the field of monocationic α -diphosphorus compounds the P–P bond is known to display both dative and covalent characters, illustrated by forms **I'** and **I''** according to the classical Lewis formalism.

Phosphonium ligands can be divided into two main classes: (i) those where the phosphorus atom is stabilized by π -donor substituents [2b,5b–g,6] such as amino substituents $(R_2N)_2P^+$ and (ii) those bound to two aryl Ar_2P^+ or alkyl R_2P^+ substituents [4,5a]. The former can be isolated as base-free phosphonium cations which may explain why extensive experimental and theoretical studies [7] have appeared since their discovery. Diaryl- and dialkyl-phosphoniums are usually prepared by halide abstraction from their corresponding halophosphane precursors and stabilized by the coordination of a Lewis base [4,5a]. Isolation of free diaryl- and dialkyl-phosphonium cations has to date remained elusive. Since their first identification, these phosphoniums have been experimentally under-explored, except the diphenylphosphonium Lewis acidic phosphorus center Ph_2P^+ . Experimental solid-state structures in conjunction with computational data indicate that

* Corresponding author. Fax: +33 5 61 55 30 03.

E-mail addresses: jean-marc.sotiro@univ-pau.fr (J.-M. Sotiropoulos), alain.igau@lcc-toulouse.fr (A. Igau).

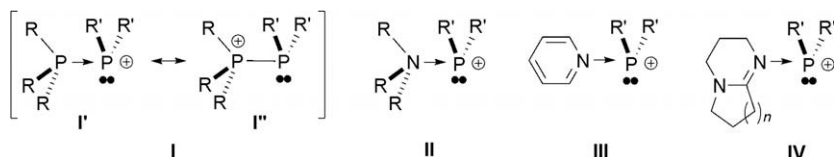


Fig. 1. Homo-PP and hetero-NP atomic *p*-block complexes with alkyl R_2P^+ and aryl Ar_2P^+ phosphonium ions as Lewis acid acceptors.

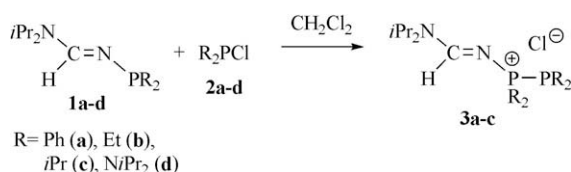
Ph_2P^+ is a better Lewis acid than its diamino phosphonium analogue $(R_2N)_2P^+$. The preparation of the first derivatives of *catena*-polyphosphorus cations from homoatomic P–P donor–acceptor aryl cations has been achieved [3b]. Very recently, diaryl- and dialkyl-phosphinophosphonium homoleptic ($R = R'$) and heteroleptic ($R \neq R'$) compounds $[R_3P-PR'_2]^+$ gave access to 1,2-diphosphonium derivatives $[R_3PPR'_3]^{2+}$ representing prototypical phosphorus analogues of ethane [3a].

While investigating the protonation reaction of the *N*-phosphino formamide (phosfam) $iPr_2N-C(H)=N-PPh_2$ **1a**, we identified the novel phosphine–phosphonium adduct, $[iPr_2N-C(H)=N-PPh_2-PPh_2]Cl$ **3a** [8]. Complex **3a** was subsequently prepared via an independent route as reported herein (Scheme 1). In this work, we expand the preparation of homoatomic homoleptic P–P derivatives $[iPr_2N-C(H)=N-PR_2-PR_2]Cl$ to $R = Et$ (**3b**) and $R = iPr$ (**3c**). We used NMR spectroscopy to explore the dynamic equilibrium $1a + 2a \rightleftharpoons 3a$ enabling the formation of a formal $P \rightarrow P$ coordinative bond (Fig. 1, I') which can also be Lewis drawn as a P–P covalent bond (Fig. 1, I''). We also report an unprecedented rearrangement which occurs with the phosfam ligand **1a** along the formation of heteroleptic ($R \neq R'$) P–P homoatomic complexes $[iPr_2N-C(H)=N-PR_2-PR'_2]Cl$. These experimental studies are supported by quantum-chemical calculations to unravel the structural and electronic properties of the formamide P–P homoatomic complexes.

2. Results and discussion

In the presence of an appropriate donor reagent, halogenophosphane compounds R_2P-Cl (**2**) are synthetic sources of the corresponding phosphonium derivatives R_2P^+ . In dichloromethane, phosfams $iPr_2N-C(H)=N-PR_2$ **1a–c** react with chlorophosphanes R_2P-Cl **2a–c** to give the corresponding homoatomic P–P donor–acceptor adducts **3a–c** in quasi quantitative yield based on ^{31}P NMR (Scheme 1). The other compound observed as a by-product in the reaction is $R_2P(O)-PR_2$ produced by the reaction of R_2P-Cl with traces of water [9]. When $R = NiPr_2$, formation of the corresponding homoatomic P–P complex $[iPr_2N-C(H)=N-P(NiPr_2)_2-P(NiPr_2)_2]Cl$ was not observed. This is most probably due to the strong covalent nature of the P–Cl bond in *P*-chlorodiamino phosphanes as they dissociate in solution only to a small extent [5b] and to the extreme steric crowding at the phosphorus atoms.

Oily solids were obtained in most attempts and crystalline or microcrystalline materials could not be obtained for **3a–c**. Nevertheless, spectroscopic features allow for definitive identification



Scheme 1. Formation of homoatomic P–P homoleptic phosphinophosphonium formamides **3a–c**.

of **3a–c**. The ^{31}P NMR chemical shifts for **3a–c** at respectively δ 31.7, 59.0, and 55.0 ppm are distinctive for the phosphonium centers and are consistent with the characteristic shift for $=N-PR_3^+$ ($\delta \approx 32$ ppm ($R = Ph$), $\delta \approx 53$ ppm ($R = iPr$)) [10]. The large $^1J_{PP}$ coupling constant values (ca. 280–340 Hz) of the new donor–acceptor adducts **3a–c** fall in the range for P–P complexes of type I reported in the literature [4a,c,e] (Fig. 1). The 1H and ^{13}C NMR spectra of **3a–c** showed the presence of the proton and the carbon of the formamide framework $>N-C(H)=N$ in the range of 8.40–8.80 ppm and 156–161 ppm respectively. The low $^2J_{CP}$ observed between the imino carbon atom and the phosphorus fragment ($2.5 < ^2J_{CP} < 7.5$ Hz) is characteristic for tetracoordinated σ^4-P *N*-phosphorus formamidino derivatives [8,10]. 2D HMBC $^1H-^{15}N$ and HMQC $^{31}P-^{15}N\{^1H\}$ NMR experiments monitored on **3a** (δ ^{31}P 31.7 and -17.6 ppm) allowed to identify the imino nitrogen atom of the formamide fragment at δ ^{15}N -244.0 ($^1J_{NP} = 51.0$ Hz) ppm which correlates with the phosphorus atom at δ ^{31}P 31.0 ppm (Fig. 2). All these NMR data suggest that the homoatomic P–P derivatives **3a–c** are best described by a covalent ‘phosphinophosphonium’ structure illustrated by I'' (Fig. 1).

Phosphonium cations R_2P^+ generated from their halophosphane precursors R_2P-Cl **2a–c**, are formally related to their synthons via a dynamic equilibrium whose position depends intimately upon the nature of the counter ion, the *R* groups coordinated to phosphorus and to some extent the solvents. In solution P–Cl bonds in alkyl and aryl R_2P-Cl species may be described as covalently interacting ion pairs or separated ions depending on the experimental reaction conditions. The formation of adduct **3a** at 293 K was tested in different solvents from the protonic and non-protonic slightly polar solvents as toluene, $CHCl_3$, CH_2Cl_2 , and THF to the highly polar CH_3CN solvent (Scheme 2). According to ^{31}P NMR, at 293 K, the major species present in THF and toluene are the *N*-phosphino formamide derivative **1a** and Ph_2P-Cl **2a**. The broad resonances are consistent with a dynamic equilibrium with **3a** which is in the

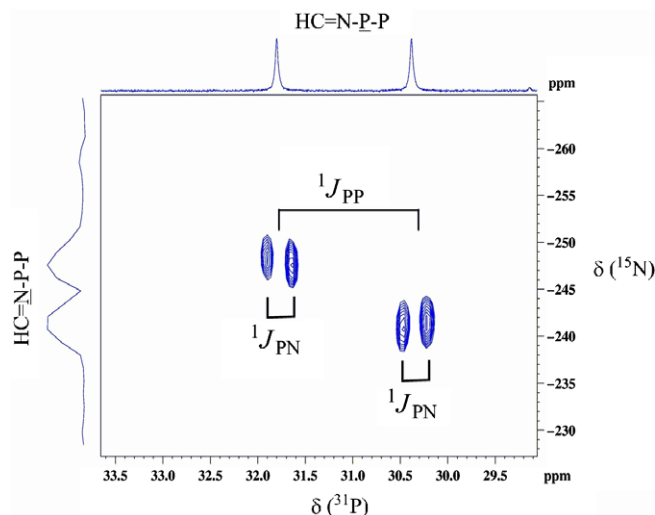
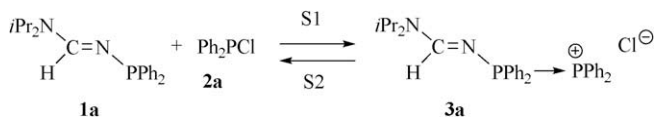


Fig. 2. 2D HMQC-nd $^{31}P-^{15}N\{^1H\}$ NMR spectrum showing correlations between phosphorus and imino nitrogen atoms in $[iPr_2N-C(H)=N-PPh_2-PPh_2]Cl$ **3a**.



Scheme 2. Solvent-dependent formation of homoatomic P–P adduct **3a** at 293 K (S1 = CH₂Cl₂, CHCl₃, CH₃CN; S2 = toluene, THF).

intermediate range on the NMR timescale. At the same temperature, in CHCl₃, CH₂Cl₂ and CH₃CN, the major species is the adduct **3a**. The large resonances suggest a rapid equilibrium between **3a** and the free species **1a** and **2a**, which is shifted almost completely towards the formation of adduct **3a**. There is undoubtedly a close connection between phosphonium reactivity and the nature of the solvent employed in the formation of **3a** in solution. It seems likely that the trend of the formation of **3a** in condensed phases arises from the interplay of several competing factors (e.g., Coulombic, directional, inductive, dispersion and hydrogen bonding interaction forces) [11] rather than from a single dominant interaction.

Variable-temperature ³¹P NMR experiments recorded in THF in the range of 293–193 K exhibited a pronounced temperature-dependent equilibrium between the phospham **1a**, Ph₂P(O)Cl **2a**, and **3a**. At 293 K the major species present are the dissociated **1a** and Ph₂P(O)Cl **2a** phosphorus derivatives as the two phosphorus resonances are close to the corresponding free species. However, the line-shapes of the signals of these species are broad, especially the one of Ph₂P(O)Cl **2a**, which is characteristic of the existence of an equilibrium. At 193 K, the major species is the donor–acceptor adduct **3a**. The formation of this complex is illustrated by the chemical shift of the Ph₂P fragment (δ ³¹P of free Ph₂P(O)Cl **2a** = 82 ppm) shielded to high field by 100 ppm (δ ³¹P (Ph₂P–) = –17.6 ppm) and the large P–P coupling constant value (¹J_{PP} = 282.5 Hz). At 243 K, the spectrum shows two broad signals at 39.4 ($\Delta\nu_{1/2}$ = 650 Hz) ppm and ~–3.0 ($\Delta\nu_{1/2}$ = 4000 Hz) ppm. These signals are close to an average position between the resonances of the donor–acceptor adduct **3a** and the dissociated **1a** and **2a** species.

Fig. 3b displays simulations of the spectra obtained at different temperatures with the WINDNMR software [12]. The model totally validates the hypothesis of a concomitant change of the **1a**:**2a**:**3a** ratio. From the DNMR simulation we were able to establish the rate of exchange between the different species **1a**, **2a**, and **3a**. An Eyring analysis over the temperature range 193–293 K afforded activation parameters of $\Delta S^{\ddagger} = (-130 \pm 7.2) \text{ J mol}^{-1} \text{ K}^{-1}$, $\Delta H^{\ddagger} = (8.4 \pm 0.6) \text{ kJ mol}^{-1}$, and $\Delta G^{\ddagger} (298.15 \text{ K}) = (53.6 \pm 2.3) \text{ kJ mol}^{-1}$. The negative entropy of activation is consistent with an associative pathway and the small value of ΔH^{\ddagger} suggests that the energy barrier for this reaction is entropically controlled. All attempts to measure analogous data using other P–P adducts were unsuccessful. However, the characteristic broadness of the ³¹P–{¹H} NMR signals associated with free and coordinated species is observed in all samples, suggesting that exchange is rapid whatever the R substituents.

We extended the formation of P–P compounds to the preparation of heteroleptic *N*-phosphino formamide complexes. The phospham **1a** was reacted at 293 K in CH₂Cl₂ with Et₂P(O)Cl **2b** to give the heteroleptic phosphinophosphonium derivative **3d** (Scheme 3). Only traces of Ph₂P(O)–PPh₂ were observed as the unique side product of the reaction.

In the ³¹P NMR spectrum of the reaction mixture, the initial chemical shifts at 54.3 ppm (**1a**) and 118.1 ppm (**2b**) are replaced by two doublets centered at 50.5 and –27.2 ppm (**3d**) with a coupling constant value ¹J_{PP} = 279.5 Hz consistent with P–P homoatomic adducts [4a,c,e]. The ¹H and ¹³C NMR spectra of **3d** showed the presence of the proton (δ 8.10 ppm, ³J_{HPEt} = 20.6 Hz) and the carbon (δ 159.0 ppm) of the formamide framework >N–C(H)=N. The absence of a ²J_{CP} coupling constant was already observed in tetracoordinated *N*-phosphorus formamide derivatives [10]. A combination of 2D homo- and heteronuclear NMR experiments with selective ³¹P decoupling allowed complete assignments of the atoms connectivity profile for the formamide phosphinophosphonium framework molecule **3d**. 2D HSQC ¹H–¹³C and HMBC ¹H–³¹P NMR experiments allowed us to assign the ethyl groups attached to the phosphorus atom at δ ³¹P 50.5 ppm. 2D HMBC ¹H–¹⁵N and HMQC ³¹P–¹⁵N{¹H} NMR experiments moni-

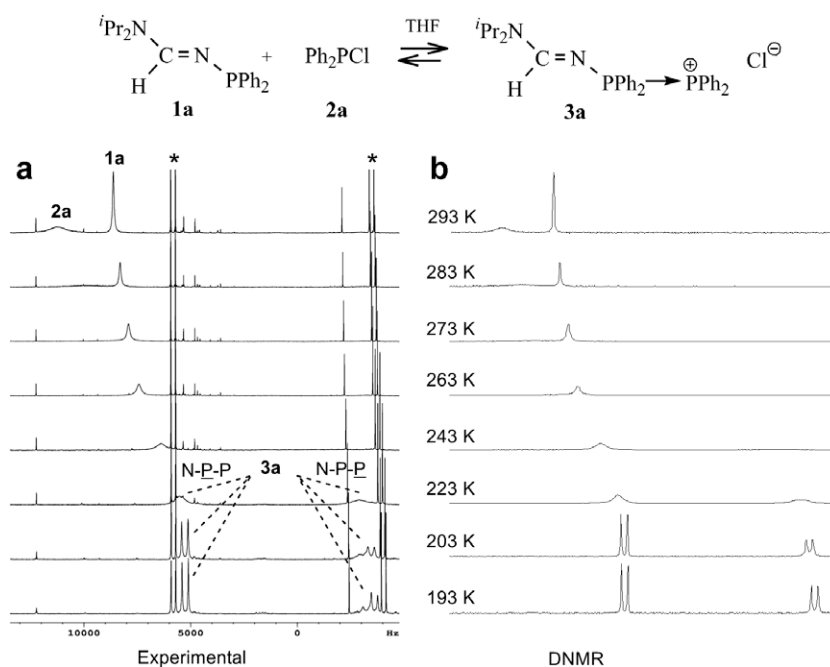
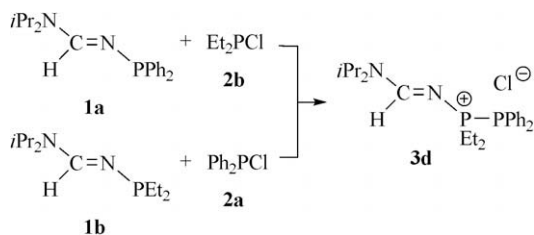


Fig. 3. (a) Experimental and (b) simulated variable-temperature ³¹P NMR experiments showing the equilibrium between the adduct **3a** and the free **1a** and Ph₂P(O)Cl **2a** species (*Ph₂PP(O)Ph₂).



Scheme 3. Formation of the homoatomic heteroleptic phosphinophosphonium formamidines **3d**.

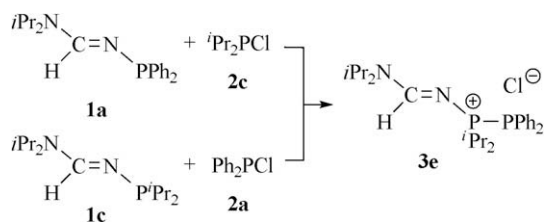
tored on **3d** allowed to identify the imino nitrogen atom of the formamidines framework at -237.7 ppm and to show the correlation with the phosphorus atom at $\delta^{31}\text{P}$ 50.5 ppm. The $^1J_{\text{NP}(\text{Et}_2)}$ coupling constant value of 50.5 Hz definitely confirmed the presence of the diethyl phosphino group directly connected to the formamidines fragment. The formation of the phosphinophosphonium **3d** results from the formal insertion reaction of Et_2P^+ into the phosphorus–nitrogen bond N–PPh₂ of the starting donor *N*-phosphino formamidines **1a**. Interestingly, the heteroleptic P–P compound **3d** was also prepared when **1b** was reacted with **2a** (Scheme 3).

The same type of rearrangement was observed when **1a** was reacted with **2c** to give the phosphinophosphonium compound **3e**, which formally resulted from the insertion reaction of $i\text{Pr}_2\text{P}^+$ into the phosphorus–nitrogen bond N–PPh₂ of the starting donor *N*-phosphino formamidines **1a** (Scheme 4). Starting from the *N*-phosphino formamidines **1c** and after addition of Ph₂P-Cl **2a** formation of the thermodynamic stable heteroleptic P–P adduct **3e** was observed (Scheme 4).

The ^{31}P NMR spectrum of **3e** showed two doublets at 52.4 and -31.5 ppm with a $^1J_{\text{PP}} = 311.2$ Hz. The isopropyl substituents are connected to the phosphorus atom resonating at $\delta^{31}\text{P}$ 52.4 ppm which is coupled to the proton of the formamidines skeleton $>\text{N}-\text{C}(\text{H})=\text{N}$ at δ 7.50 ($^3J_{\text{HP}(\text{iPr}_2)} = 18.8$ Hz) ppm. The $^1J_{\text{NP}(\text{iPr}_2)}$ coupling constant value of 51.8 Hz of the imino nitrogen atom at -238.1 ppm definitely confirmed the presence of the diisopropyl phosphino group directly attached to the formamidines fragment.

In order to have a better insight into the geometrical and electronic structures of the *N*-phosphino formamidines complexes **3a–c**, DFT calculations at the B3LYP/6-31G** level of theory were carried out. In agreement with the experimental data, the formamidines homoatomic P–P derivatives were found as global minima on the potential energy surface. The *E* configuration corresponds to the most thermodynamically stable structure in which the P–P bond and the imino nitrogen lone pair are in *trans* position, except for **3a** where the P–P–C–N dihedral angle value is 106° (Fig. 4). The main geometrical parameters for **3a–c** are shown in Table 1.

The calculated C1–N1 bond lengths of ≈ 1.31 Å in **3a–c** are slightly longer than those observed in **1a–c** [8] (*vide infra*) and fall in the upper limit for double carbon–nitrogen bond [13]. This C1–N1 bond length elongation is commonly observed for tetracoordinated *N*-phosphonium formamidines derivatives [10] and results



Scheme 4. Formation of the homoatomic heteroleptic phosphinophosphonium formamidines **3e**.

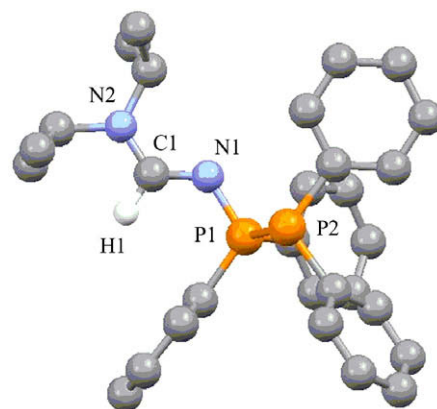


Fig. 4. Molekel plot of the calculated molecular structure of **3a** with hydrogen atoms omitted and numbering atoms.

Table 1

Selected calculated bond lengths (Å) and angles ($^\circ$) for **3a–c**. NPA charges (q_x).

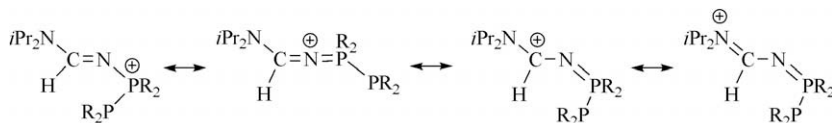
X	3a	3b	3c
C1–N1	1.312	1.316	1.314
N1–P1	1.656	1.649	1.655
P1–P2	2.261	2.248	2.261
N1–P1–P2	103.81	111.74	111.83
C1–N1–P1	123.03	124.93	125.63
$\Delta G_{\text{reaction}}^a$	-27.4	-53.4	-36.7
q_{N1}	-0.97	-0.98	-0.98
q_{P1}	1.54	1.51	1.51
q_{P2}	0.65	0.56	0.55

^a Calculated energies in kcal mol^{-1} for the reaction '**2a–c** + R_2P^+ \rightarrow **3a–c**'.

from a partial delocalization of the positive charge along the formamidines framework (Scheme 5).

The N1–P1 bond lengths of ≈ 1.65 Å in **3a–c** are considerably shorter than those in the corresponding phosphams **1a–c** (≈ 1.75 Å) and the phosphorus–phosphorus bond lengths (~ 2.25 Å) are in the range of those reported for P–P donor–acceptor adducts [4c,e]. The CNP bond angles are around 125° . Besides the strong stabilizing interaction between the P amino nitrogen lone pair and the $\pi_{\text{C}=\text{N}}$ orbital (~ 90 kcal/mol), consistent with the delocalization, NBO calculations show significant negative hyperconjugations (~ 7.5 – 11 kcal/mol) between the imino nitrogen lone pair and $\sigma_{\text{C–H}}$ and $\sigma_{\text{P–P}}$ (or $\sigma_{\text{P–C}}$ for the phenyl substituents) orbitals, leading to a decrease of the PN bond lengths. All these stabilizing interactions are in favor for the formation of the P–P adducts. Considering the calculated $\Delta G_{\text{reaction}}$ (Table 1), it is noteworthy that the reaction is exothermic and that the calculated values are consistent with the experimental data since the driving force of the reaction is the formation of the P–P adducts. Moreover the NPA charges, obtained from the NBO analysis, are consistent with a phosphinophosphonium covalent structure (type I'') with the phosphorus atom P1 next to the imino nitrogen atom bearing a strong positive charge, $q_{\text{P1}} = 1.51$ – 1.54 , (Table 1) and the phosphorus atom P2 at the terminal position a less positive one $q_{\text{P2}} \approx 0.5$. The calculated geometrical parameters as well as the NBO analyses clearly indicate that the adducts **3a–c** can be represented by the phosphinophosphonium Lewis structure I''.

In order to provide more information on the complexes **3a–c**, the donor *N*-phosphino formamidines **1a–c** and acceptor phosphonium cations R_2P^+ (R = Ph, Et, *iPr*) were theoretically studied. As previously reported [8] for the phosphams $i\text{Pr}_2\text{N}-\text{C}(\text{H})=\text{N}-\text{PR}_2$ **1a,c**, for R = Et, the *E* configuration corresponds to the most thermodynamically stable structure in which the imino nitrogen and phos-



Scheme 5. Mesomeric forms in the formamidine framework of the phosphinophosphonium **3**.

phorus lone pairs are in *trans* position. The C=N and P–N bond lengths are respectively about 1.29 Å and 1.75 Å. The phosphorus and imino nitrogen charges are similar for all the compounds. The energetic positions of the bonding combination ($n_p + n_N$) with an important weight on phosphorus vary from -5.1 to -5.3 eV and from -7.1 to -7.8 eV for the antibonding combination ($n_p - n_N$) with an important weight on imino nitrogen (Table 2).

In the determination of acceptor properties of the free phosphonium cations R_2P^+ ($R = Ph, Et, iPr$), the most important frontier orbital is the lowest unoccupied molecular $3p^\pi(P)$ orbital (LUMO). Table 3 summarizes the main geometrical parameters, the energetic positions of the HOMO [$n^\sigma(P)$] and the LUMO [$3p^\pi(P)$], the NPA charges and the $3p^\pi(P)$ occupation for the two alkyl ($R = Et, iPr$) and aryl (Ph) substituents.

The results are consistent with those previously reported by Macdonald et al. [14] for the diphenyl and dimethylamino phosphonium cations. The P–C bond lengths vary from 1.77 Å to 1.85 Å ($Ph_2P^+ > Et_2P^+ > iPr_2P^+$) and the C–P–C angles from 104 to 109.5°. It is noteworthy that the two P–C bond lengths are surprisingly inequivalent with *iPr* substituents. The energetic position of the most accessible $3p^\pi(P)$ orbital depends on the substituents and reflects their electron acceptor ability (Fig. 5). The $3p^\pi(P)$ orbitals

are relatively close for the Ph_2P^+ (-8.07 eV) and iPr_2P^+ (-7.56 eV) cations, whereas the LUMO (-9.62 eV) of Et_2P^+ is more accessible by about 1.5 eV. The distinct difference observed between the phosphonium cations can be explained by strong interactions between the σ_{CH} and σ_{CH}/σ_{CC} orbitals and the $3p^\pi(P)$ orbital respectively for Et_2P^+ and iPr_2P^+ (Table 3), which destabilize the unoccupied phosphorus p orbital.

In addition to the orbital consideration, the π -acceptor effect in the phosphonium species R_2P^+ ($R = Ph, Et, iPr$) can be estimated by regarding the electron population in the $3p^\pi(P)$ orbital. The NBO analysis indicates that the occupation in iPr_2P^+ is slightly more important than the one in Et_2P^+ . For the phenyl cation Ph_2P^+ a higher occupation of the phosphorus $3p^\pi$ orbital is observed in comparison with the alkyl analogues, illustrating a slight π -delocalization. Nevertheless the lowest energy structure found for Ph_2P^+ shows non coplanar phenyl substituents, limiting the corresponding MO overlap. In this case, the energetic position of the $3p^\pi(P)$ orbital is intermediate between those of the two alkyl substituents because of interaction between this latter orbital and one of the $\pi_{C=C}$ orbitals of the phenyl ring, leading to a stabilization of the unoccupied p phosphorus orbital. Consequently, the bis(ethyl)phosphonium cation is the best acceptor of this series.

Overall, the formation of the heteroleptic P–P compounds **3d** and **3e** starting from the phosfam ligand **1a** and the corresponding phosphonium precursors **2b** and **2c**, respectively, cannot be rationalized from the strict consideration of the position of the molecular orbitals in donor derivatives **1a–c** and acceptor phosphonium cations R_2P^+ ($R = Ph, Et, iPr$). From the computed data it is evident that the charges should have a decisive contribution in the formation of phosphinophosphonium formamidines **3d,e**. Consequently, the imino nitrogen of the formamidine fragment may interact with the Lewis acid phosphorus center of the phosphonium cations during the course of the reaction. In fact, on the potential energy surface, we found that the heteroatomic N–P formamidine isomer [$iPr_2N-C(H)=N(PR_2)PR_2$] $^+$ exists as a minimum, which is thermodynamically less stable than the corresponding homoatomic P–P formamidine [$iPr_2N-C(H)=N-PR_2-PR_2$] $^+$ compound with an energetic difference in the range of 15–25 kcal mol $^{-1}$ (see Supplementary material). Moreover, a transition state has been located on the potential energy surface with an energy barrier allowing the heteroatomic N–P (**4**)/homoatomic P–P (**3**) rearrangement. This rearrangement energy profile has been computed with alkyl substituents in order to reduce calculation time. In the gas phase, for $R = R' = Et, iPr$, the value of the energetic barrier for the heteroatomic/homoatomic rearrangement ranges from 22 to 30 kcal mol $^{-1}$ (see Supplementary material). Overall, considering the experimental (condensed phase) and computed data (gas phase), it is reasonable to propose in a first step the formation of the transient heteroatomic N–P intermediates [$iPr_2N-C(H)=N(PR_2)PR_2$] $^+$ which then rearrange to the corresponding more thermodynamically stable P–P formamidine adducts **3** (Scheme 6).

The heteroatomic N–P intermediates [$iPr_2N-C(H)=N(PR_2)PR_2$] $^+$ may be represented by several mesomeric Lewis structures such as the formamidinium species **4A** or **4B**. Theoretical calculations have evidenced that the preparation of compounds **3** goes through the formation of a 3-membered transition state **5**.

Table 2

Selected calculated bond lengths (Å) and angles (°) for *N*-phosphino formamidine **1a–c** at the B3LYP/6-31G** level. NPA charges (q_N). Energetic positions (eV) of the bonding and antibonding P and N lone pair combination, calculated at the B3LYP/6-31G** and MP2/6-31G** level of theory.

X	1a	1b	1c
C1–N1	1.293	1.292	1.292
P1–N1	1.737	1.746	1.746
C1–N1–P1	115.56	116.13	116.13
q_{N1}	–0.89	–0.89	–0.89
q_{P1}	1.03	1.00	1.00
($n_p + n_N$) B3LYP	–5.33	–5.12	–5.10
($n_p + n_N$) MP2	–8.00	–8.14	–8.01
($n_p + n_N$) B3LYP	–7.78	–7.21	–7.13
($n_p + n_N$) MP2	–11.46	–10.99	–10.90

Table 3

Selected calculated bond lengths (Å) and angles (°) for the phosphonium cations R_2P^+ ($R = Ph, Et, iPr$) at the B3LYP/6-31G** level. Energetic positions (eV) of the frontier orbitals calculated at the B3LYP/6-31G** and MP2/6-31G** level of theory. Phosphorus NPA charges (q_P), occupation of the $3p^\pi(P)$ and main stabilizing interactions (Kcal mol $^{-1}$) involving the $3p^\pi(P)$ orbital.

X	Ph_2P^+	Et_2P^+	iPr_2P^+
P–C	1.766	1.801	1.846/1.824
C–P–C	104.08	103.72	109.42
q_P	1.07	0.24	0.32
Pop. $3p^\pi(P)$	0.58	1.31	1.15
E_{HOMO}	–12.15	–13.28	–12.53
E_{LUMO}^{MP2}	–8.07	–9.62	–7.56
E_{LUMO}	–4.98	–5.84	–3.67
Main stabilizing interactions (Kcal mol $^{-1}$)	$\pi_{C=C}^{ph1} \rightarrow 3p^\pi(P)$: 54.5	$\sigma_{CH} \rightarrow 3p^\pi(P)$: 16.1	$\sigma_{CH} \rightarrow 3p^\pi(P)$: 64.5
	$\pi_{C=C}^{ph2} \rightarrow 3p^\pi(P)$: 54.6		$\sigma_{CC} \rightarrow 3p^\pi(P)$: 25.7

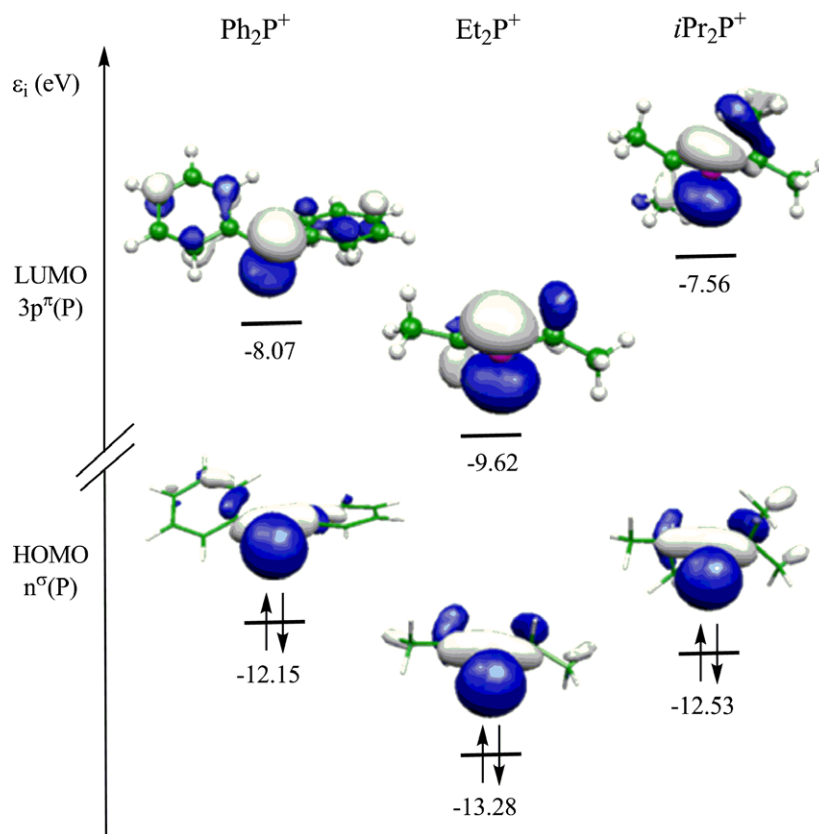
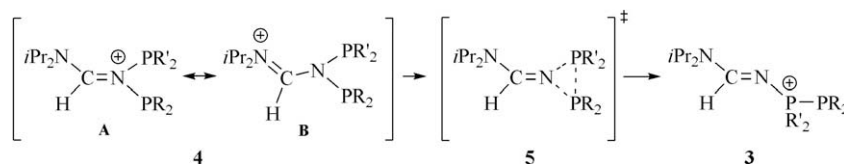


Fig. 5. Molekel plots and energetic positions (Kohn-Sham energies in eV) of the LUMO and HOMO for phosphonium species R_2P^+ with $R = Ph, Et, iPr$.



Scheme 6. Proposed mechanism for the formation of P-P homoatomic phosphinophosphonium formamidines **3**.

3. Conclusions

In the present study we report the preparation of a series of homoatomic P-P homoleptic ($R = R' = Ph, Et, iPr$) and heteroleptic ($R = Et, R' = Ph$; and $R = iPr, R' = Ph$) *N*-phosphino formamidine complexes $[iPr_2N-C(H)=N-PR_2-PR'_2]Cl$. We have demonstrated that changing the solvent or the temperature allowed to control the formation of the $[iPr_2N-C(H)=N-PPh_2-PPh_2]Cl$ adduct. The phosphonium cations R_2P^+ in the presence of the *N*-phosphino formamidine (phosfam) donor derivatives give the corresponding electron pair donor (EPD)-electron pair acceptor (EPA) complexes. The dynamic equilibrium observed in the different condensed phases involves P-P dissociation in $[iPr_2N-C(H)=N-PR_2-PR'_2]Cl$ adducts. The unprecedented rearrangement which occurs along the formation of the homoatomic P-P heteroleptic ($R = Et, iPr$; $R' = Ph$) complexes $[iPr_2N-C(H)=N-PR_2-PR'_2]Cl$ results in the formal insertion of the phosphino group of the corresponding alkyl chlorophosphanes R_2PCl into the N-P bond of the starting phosfam ligand $iPr_2N-C(H)=N-PPh_2$. Phosphine-phosphonium illustrated by **1'** is the most appropriate term to describe the dynamic process observed at variable temperature for complexes $[iPr_2N-C(H)=N-PR_2 \rightarrow PR'_2]^+$, but the ^{31}P NMR chemical shift and the calculated

electronic charges are more in favor of the phosphinophosphonium covalent Lewis drawing $[iPr_2N-C(H)=N-PR_2-PR'_2]^+$ illustrated by form **1'**. Computed data are in agreement with the proposed transient formation of a heteroatomic N-P intermediate $[iPr_2N-C(H)=N(PR_2)PR'_2]Cl$ illustrated by **4**, which then rearranges to the more thermodynamically favored homoatomic P-P formamidine compound $[iPr_2N-C(H)=N-PR_2-PR'_2]Cl$ **3**.

4. Experimental

4.1. General

All reactions were conducted under an inert atmosphere of dry argon using standard Schlenk-line techniques. Chemicals were treated as follows: pentane and CH_2Cl_2 distilled from CaH_2 ; $CDCl_3$ distilled from P_2O_5 ; C_6D_6 , CD_2Cl_2 (Euriso-top) and other solvents stored on 4 Å molecular sieves. Solvents were degassed by standard methods before use. Chlorodiphenylphosphane (97%) was obtained from ALFA AESAR and distilled prior to use. All other commercial chemicals were from Aldrich (*N,N*-diisopropylcyanamide, 97%), ACROS (chlorodiisopropylphosphane, 96%) and STREAM (bis(cyclopentadienyl)zirconium dichloride, 99%) and were used as

received. $[\text{Cp}_2\text{ZrHCl}]_n$ was prepared following the procedure reported by Buchwald et al. [15]. Infrared spectra were performed in solution (KBr windows) on a Perkin–Elmer GX 2000 spectrometer. Mass spectra were recorded on a TSQ7000 Thermo Electron (EI) and on a Q Trap (ES–MS) mass spectrometer. Melting points were obtained using an Electrothermal Digital Melting Point apparatus and are uncorrected. Elemental analyses were carried out by the “Service d’Analyse du Laboratoire de Chimie de Coordination” in Toulouse.

4.2. NMR experiments

^1H , $^1\text{H}\text{--}\{^3\text{P}\}$, $^3\text{P}\text{--}\{^1\text{H}\}$, $^{13}\text{C}\text{--}\{^1\text{H}\}$ and $^{13}\text{C}\text{--}\{^1\text{H}, ^3\text{P}\}$ NMR spectra were recorded on a Bruker AV500, AV 400, and AV 300 spectrometers equipped with a 5 mm triple resonance inverse probe with dedicated ^3P channel. All chemical shifts for ^1H and ^{13}C are relative to TMS using residual peak of the solvent as a secondary standard. ^3P chemical shifts were referenced to an external 85% H_3PO_4 sample. The ^{15}N resonances were referenced to neat CH_3NO_2 . Temperature calibration was determined using a methanol chemical shift thermometer. All the ^1H and ^{13}C signals were assigned on the basis of chemical shifts, spin–spin coupling constants, splitting patterns and signal intensities, and by using 2D $^1\text{H}\text{--}^1\text{H}$ COSY45, $^1\text{H}\text{--}^{13}\text{C}$ HSQC, $^1\text{H}\text{--}^{13}\text{C}$ HMBC, $^1\text{H}\text{--}^{15}\text{N}$ HMBC and $^3\text{P}\text{--}^{15}\text{N}$ HMQC- $\{^1\text{H}\}$ with broadband or selective ^3P decoupling when necessary. All spectra were recorded at ambient probe temperature unless stated otherwise. NMR simulations were run with WINDNMR-Pro 7.1.12 software [12].

4.3. Preparation of *N*-phosphino formamidines $i\text{Pr}_2\text{NC}(\text{H})=\text{NPET}_2$ (**1b**)

Following the procedure described for **1a**, **c** [8], **1b** and **1d** were prepared after addition of a solution of $i\text{Pr}_2\text{NCN}$ (7.814 mmol) in CH_2Cl_2 (5 mL) to a suspension of $[\text{Cp}_2\text{Zr}(\text{H})\text{Cl}]_n$ (7.814 mmol) in CH_2Cl_2 (15 mL) followed by $\text{Et}_2\text{P}(\text{Cl})$ and $(i\text{Pr}_2\text{N})_2\text{P}(\text{Cl})$ respectively (7.814 mmol) to give **1b** in 85% yield (1.436 g, 6.642 mmol) and **1d** in 90% yield (2.502 g, 6.989 mmol). **1b**: IR (KBr, THF): ν ($\text{C}=\text{N}$) = 1607 cm^{-1} . ^3P NMR (121 MHz, C_6D_6): $[\delta/\text{ppm}]$ 91.0 (s). ^1H NMR (300 MHz, CD_2Cl_2): $[\delta/\text{ppm}]$ 7.95 (d, 1H, $^3J_{\text{HP}} = 19.1$ Hz, $\text{HC}=\text{N}$), 4.56 (m, 1H, NCHCH_3), 3.52 (m, 1H, NCHCH_3), 1.42 (m, 4H, PCH_2CH_3), 1.35 (d, 6H, $^3J_{\text{HH}} = 6.8$ Hz, NCHCH_3), 1.32 (d, 6H, $^3J_{\text{HH}} = 6.7$ Hz, NCHCH_3), 0.99 (td, 6H, $^3J_{\text{HP}} = 14.8$ Hz, $^3J_{\text{HH}} = 7.5$ Hz, PCH_2CH_3). ^{13}C NMR (75 MHz, CD_2Cl_2): $[\delta/\text{ppm}]$ 157.1 (d, $^2J_{\text{CP}} = 47.4$ Hz, $\text{HC}=\text{N}$), 50.3 (s, NCHCH_3), 47.1 (s, NCHCH_3), 23.2 (s, NCHCH_3), 19.7 (s, NCHCH_3), 25.3 (d, $^2J_{\text{CP}} = 8.8$ Hz, PCH_2CH_3), 9.0 (d, $^2J_{\text{CP}} = 13.5$ Hz, PCH_2CH_3). EI MS m/z (%): 216 [M^+]. $\text{C}_{11}\text{H}_{25}\text{N}_2\text{P}$: calcd. C 61.08, H 11.65, N 12.95; found C, 61.96, H 12.08, N 12.48.

Compound **1d**: IR (KBr, THF): ν ($\text{C}=\text{N}$) = 1602 cm^{-1} . ^3P NMR (121 MHz, C_6D_6): $[\delta/\text{ppm}]$ 71.3 (s). ^1H NMR (300 MHz, CD_2Cl_2): $[\delta/\text{ppm}]$ 8.14 (d, 1H, $^3J_{\text{HP}} = 18.0$ Hz, $\text{HC}=\text{N}$), 4.72 (m, 1H, NCHCH_3), 3.92 (d sept; 4H, $^3J_{\text{HH}} = 6.7$ Hz; $^3J_{\text{HP}} = 10.4$ Hz; PNCHCH_3), 3.11 (m, 1H, NCHCH_3), 1.48 (d; 12H; $^3J_{\text{HH}} = 6.7$ Hz; PNCHCH_3), 1.44 (d; 12H; $^3J_{\text{HH}} = 6.7$ Hz; PNCHCH_3), 1.19 (m, 6H, NCHCH_3), 0.97 (m, 6H, NCHCH_3). ^{13}C NMR (75 MHz, CD_2Cl_2): $[\delta/\text{ppm}]$ 152.3 (d, $^2J_{\text{CP}} = 65.4$ Hz, $\text{HC}=\text{N}$), 46.3 (s, NCHCH_3), 45.5 (d; $^2J_{\text{CP}} = 11.4$ Hz; PNCHCH_3), 44.5 (s, NCHCH_3), 24.9 (d, $^2J_{\text{CP}} = 8.8$ Hz, PNCHCH_3), 24.7 (d, $^3J_{\text{CP}} = 5.6$ Hz; PNCHCH_3), 24.0 (s, NCHCH_3), 20.5 (s, NCHCH_3). EI MS m/z (%): 358 [M^+]. Anal. Calc. for $\text{C}_{19}\text{H}_{43}\text{N}_4\text{P}$: C, 63.65; H, 12.09; N, 15.63. Found: C, 63.87; H, 12.23; N, 15.32%.

4.4. Representative experimental procedure for the preparation of *P*–*P* homoatomic phosphinophosphonium formamidines $[i\text{Pr}_2\text{N}\text{--}\text{C}(\text{H})=\text{N}\text{--}\text{PR}_2\text{--}\text{PR}_2]\text{Cl}$ (**3a–e**)

A Schlenk flask was charged with $i\text{Pr}_2\text{N}\text{--}\text{C}(\text{H})=\text{N}\text{--}\text{PPh}_2$ (**1a**, 0.151 g, 0.480 mmol), $\text{Ph}_2\text{P}(\text{Cl})$ (**2a**, 0.106 g, 0.480 mmol) and CH_2Cl_2

(5 mL). The mixture was stirred for 5 min. The solvent was removed by oil pump vacuum to give **3a** in quasi quantitative yield as a white residue (0.256 g, 0.480 mmol). Compound **3a** was characterized by NMR without any further treatment. ^3P NMR (81 MHz, CDCl_3): $[\delta/\text{ppm}]$ 31.7 (d, $^1J_{\text{PP}} = 282.5$ Hz, $\text{N}\text{--}\text{P}\text{--}\text{P}$), -17.6 (d, $^1J_{\text{PP}} = 282.5$ Hz, $\text{N}\text{--}\text{P}\text{--}\text{P}$). ^1H NMR (200 MHz, CDCl_3): $[\delta/\text{ppm}]$ 7.58–7.03 (m, 21H, H_{Ph} and $\text{HC}=\text{N}$), 4.37 (sept, 1H, $^3J_{\text{HH}} = 6.8$ Hz, NCHCH_3), 3.54 (sept, 1H, $^3J_{\text{HH}} = 6.7$ Hz, NCHCH_3), 1.12 (d, 6H, $^3J_{\text{HH}} = 6.8$ Hz, NCHCH_3), 0.92 (d, 6H, $^3J_{\text{HH}} = 6.7$ Hz, NCHCH_3). ^{13}C NMR (50 MHz, CDCl_3): $[\delta/\text{ppm}]$ 156.5 (d, $^2J_{\text{CP}} = 3.4$ Hz, $\text{HC}=\text{N}$), 135.1 (d, $^1J_{\text{CP}} = 7.0$ Hz, $i\text{-PC}_{\text{Ph}}$), 134.7 (d, $^1J_{\text{CP}} = 10.4$ Hz, $i\text{-PC}_{\text{Ph}}$), 134.5 (s, CH_{Ph}), 134.2 (s, CH_{Ph}), 131.9 (d, $J_{\text{CP}} = 8.8$ Hz, CH_{Ph}), 131.3 (s, CH_{Ph}), 129.7 (d, $J_{\text{CP}} = 11.8$ Hz, CH_{Ph}), 129.3 (d, $J_{\text{CP}} = 7.3$ Hz, CH_{Ph}), 50.1 (s, NCHCH_3), 47.8 (s, NCHCH_3), 23.1 (s, NCHCH_3), 19.3 (s, NCHCH_3). ^{15}N NMR (51 MHz, [toluene- d_8]): $[\delta/\text{ppm}]$ -210.0 ($\text{N}^{\text{Pr}2}$), -244.0 ($^1J_{\text{NP}} = 51.0$ Hz, $\text{C}=\text{N}\text{--}\text{P}$).

Compound **3b**: ^3P NMR (81 MHz, CDCl_3): $[\delta/\text{ppm}]$ 55.5 (d, $^1J_{\text{PP}} = 281.8$ Hz, $\text{N}\text{--}\text{P}\text{--}\text{P}$), -36.7 (d, $^1J_{\text{PP}} = 281.8$ Hz, $\text{N}\text{--}\text{P}\text{--}\text{P}$). ^1H NMR (200 MHz, CDCl_3): $[\delta/\text{ppm}]$ 8.75 (d, 1H, $^3J_{\text{HP}} = 20.8$ Hz, $\text{HC}=\text{N}$), 4.41 (sept, 1H, $^3J_{\text{HH}} = 6.8$ Hz, NCHCH_3), 3.99 (sept, 1H, $^3J_{\text{HH}} = 6.8$ Hz, NCHCH_3), 3.52 (m, 2H, PCH_2CH_3), 2.47 (m, 2H, PCH_2CH_3), 1.97 (m, 2H, PCH_2CH_3), 1.76 (m, 2H, PCH_2CH_3), 1.14–1.42 (m, 24H, NCHCH_3 et PCH_2CH_3). ^{13}C NMR (50 MHz, CDCl_3): $[\delta/\text{ppm}]$ 160.2 (d, $^2J_{\text{CP}} = 2.5$ Hz, $\text{HC}=\text{N}$), 50.7 (s, NCHCH_3), 46.9 (s, NCHCH_3), 22.9 (s, NCHCH_3), 19.8 (s, NCHCH_3), 18.0 (dd, $J_{\text{C,P}} = 47.6$ Hz, $J_{\text{CP}} = 8.0$ Hz, NPCH_2CH_3), 14.1 (dd, $J_{\text{CP}} = 17.2$ Hz, $J_{\text{CP}} = 2.9$ Hz, PPCH_2CH_3), 11.7 (dd, $J_{\text{CP}} = 17.0$ Hz, $J_{\text{C,P}} = 9.8$ Hz, PPCH_2CH_3), 11.7 (dd, $J_{\text{CP}} = 17.0$ Hz, $J_{\text{CP}} = 9.8$ Hz, PPCH_2CH_3), 6.4 (dd, $J_{\text{CP}} = 5.5$ Hz; $J_{\text{CP}} = 5.5$ Hz; NPCH_2CH_3).

Compound **3c**: ^3P NMR (81 MHz, CD_2Cl_2): $[\delta/\text{ppm}]$ 59.0 (d, $^1J_{\text{PP}} = 340.9$ Hz, $\text{N}\text{--}\text{P}\text{--}\text{P}$), -6.2 (d, $^1J_{\text{PP}} = 340.9$ Hz, $\text{N}\text{--}\text{P}\text{--}\text{P}$). ^1H NMR (200 MHz, CD_2Cl_2): $[\delta/\text{ppm}]$ 8.42 (d, 1H, $^3J_{\text{HP}} = 19.3$ Hz, $\text{HC}=\text{N}$), 4.49 (sept, 1H, $^3J_{\text{HH}} = 6.8$ Hz, NCHCH_3), 3.02 (m, 2H, PCHCH_3), 2.43 (m, 2H, PCHCH_3), 1.09–1.37 (m, 36H, CHCH_3). ^{13}C NMR (50 MHz, CD_2Cl_2): $[\delta/\text{ppm}]$ 160.4 (d, $^2J_{\text{CP}} = 7.5$ Hz, $\text{HC}=\text{N}$), 50.5 (s, NCHCH_3), 49.8 (s, NCHCH_3), 47.1 (d, $J_{\text{CP}} = 4.5$ Hz, PCHCH_3), 46.8 (d, $J_{\text{CP}} = 3.3$ Hz, PCHCH_3), 27.6 (dd, $J_{\text{CP}} = 41.7$ Hz, PCHCH_3), 23.4 (s, NCHCH_3), 21.8 (dd, $J_{\text{CP}} = 21.4$ Hz, $J_{\text{CP}} = 2.4$ Hz, PCHCH_3), 21.5 (d, $J_{\text{CP}} = 2.8$ Hz, PCHCH_3), 21.5 (s, NCHCH_3), 19.7 (d, $J_{\text{CP}} = 3.1$ Hz, PCHCH_3), 15.5 (d, $J_{\text{CP}} = 2.0$ Hz, PCHCH_3).

Compound **3d**: ^3P NMR (202 MHz, CD_2Cl_2): $[\delta/\text{ppm}]$ 50.5 (d, $^1J_{\text{PP}} = 279.5$ Hz, $\text{P}(\text{Et})_2$), -27.2 (d, $^1J_{\text{PP}} = 279.5$ Hz, $\text{P}(\text{Ph})_2$). ^1H NMR (500 MHz, CD_2Cl_2): $[\delta/\text{ppm}]$ 8.10 (d, 1H, $^3J_{\text{HP}} = 20.6$ Hz, $\text{HC}=\text{N}$), 7.72–7.49 (m, 10H, H_{Ph}), 4.36 (sept, 1H, $^3J_{\text{HH}} = 6.8$ Hz, NCHCH_3), 3.79 (sept, 1H, $^3J_{\text{HH}} = 6.8$ Hz, NCHCH_3), 2.43 (m, 4H, $^3J_{\text{HH}} = 7.8$ Hz, PCH_2CH_3), 1.21 (d, 6H, $^3J_{\text{HH}} = 6.8$ Hz, NCHCH_3), 1.20 (d, 6H, $^3J_{\text{HH}} = 6.8$ Hz, NCHCH_3), 1.19 (td, 6H, $^3J_{\text{HP}} = 18.3$ Hz, $^3J_{\text{HH}} = 7.6$ Hz, PCH_2CH_3). ^{13}C NMR (126 MHz, CD_2Cl_2): $[\delta/\text{ppm}]$ 159.0 (s, $\text{HC}=\text{N}$), 135.0 (dd, $^2J_{\text{CP}} = 21.4$ Hz, $^3J_{\text{CP}} = 6.5$ Hz, $o\text{-CH}_{\text{Ph}}$), 131.1 (s large, $^4J_{\text{CP}} < 1.0$ Hz, $^5J_{\text{CP}} = 2.3$ Hz, $p\text{-CH}_{\text{Ph}}$), 129.7 (dd, $^3J_{\text{CP}} = 8.2$ Hz, $^4J_{\text{CP}} < 2.0$ Hz, $m\text{-CH}_{\text{Ph}}$), 126.8 (dd, $^1J_{\text{CP}} = 14.8$ Hz, $^2J_{\text{CP}} = 4.0$ Hz, $i\text{-PC}_{\text{Ph}}$), 18.1 (dd, $^1J_{\text{CP}} = 48.2$ Hz, $^2J_{\text{CP}} = 10.0$ Hz, PCH_2CH_3), 6.1 (dd, $^2J_{\text{CP}} = 5.9$ Hz, $^3J_{\text{CP}} = 5.8$ Hz, PCH_2CH_3). ^{15}N NMR (51 MHz, [toluene- d_8]): $[\delta/\text{ppm}]$ -213.9 (d, $^3J_{\text{NP}} = 10.0$ Hz, $\text{N}^{\text{Pr}2}$), -237.7 (d, $^1J_{\text{NP}} = 50.5$ Hz, $\text{C}=\text{N}\text{--}\text{P}$).

Compound **3e**: ^3P NMR (202 MHz, CD_2Cl_2): $[\delta/\text{ppm}]$ 52.4 (d, $J_{\text{PP}} = 311.2$ Hz, $\text{P}^{\text{Pr}2}$), -31.5 (d, $J_{\text{PP}} = 311.2$ Hz, $\text{P}(\text{Ph})_2$). ^1H NMR (500 MHz, CD_2Cl_2): $[\delta/\text{ppm}]$ 7.50 (d, 1H, $^3J_{\text{HP}} = 18.8$ Hz, $\text{HC}=\text{N}$), 7.80–7.20 (m, 10H, H_{Ph}), 4.51 (sept, 1H, $^3J_{\text{HH}} = 6.8$ Hz, NCHCH_3), 3.63 (sept, 1H, $^3J_{\text{HH}} = 6.8$ Hz, NCHCH_3), 2.89 (sept d, 2H, $^3J_{\text{HH}} = 7.2$ Hz, $^2J_{\text{HP}} = 12.6$ Hz, PCHCH_3), 1.32 (dd, 6H, $^3J_{\text{HH}} = 7.2$ Hz, $^3J_{\text{HP}} = 17.3$ Hz, PCHCH_3), 1.30 (d, 6H, $^3J_{\text{HH}} = 6.8$ Hz, NCHCH_3), 1.24 (dd, 6H, $^3J_{\text{HH}} = 7.2$ Hz, $^3J_{\text{HP}} = 16.8$ Hz, PCHCH_3), 1.14 (d, 6H, $^3J_{\text{HH}} = 6.8$ Hz, NCHCH_3). ^{13}C NMR (126 MHz, CD_2Cl_2): $[\delta/\text{ppm}]$ 157.7 (s, $\text{HC}=\text{N}$), 136.0–126.4 (broad resonances), 50.1 (s, NCHCH_3), 47.0 (s, NCHCH_3), 27.1 (d, $^1J_{\text{CP}} = 43.7$ Hz, PCHCH_3), 22.9

(s, NCHCH₃), 19.4 (s, NCHCH₃), 17.0 (s, PCHCH₃), 16.7 (d, ²J_{CP} = 3.6 Hz, PCHCH₃). ¹⁵N NMR (51 MHz, [toluene-*d*₈]): −238.1 (d, ¹J_{NP} = 51.8 Hz, C=N–P), −213.3 (s, ³J_{NP} = 9.8 Hz, NⁱPr).

4.5. Computational details

Calculations were performed with the Gaussian 03 suite of programs [16], using the density functional method [17]. The hybrid exchange functional B3LYP in conjunction with the 6-31G** [18] basis set was used. B3LYP [19] is a three parameter functional developed by Becke which combines the Becke gradient-corrected exchange functional and the Lee–Yang–Parr and Vosko–Wilk–Nusair correlation functionals with part of exact HF exchange energy. Geometry optimisations were carried out without any symmetry restrictions, the nature of the *extrema* (*minimum or transition state*) was verified with analytical frequency calculations. All free Gibbs energies have been zero-point energy (ZPE) and temperature corrected using unscaled density functional frequencies. Natural Bond Orbital (NBO) [20] analysis was used to calculate the natural charges, determine the stabilizing interactions and the occupancy of the 3p^πP orbital. Molecular Orbitals have been plotted with the Molekel package [21].

Acknowledgements

We thank the CNRS for financial support and the Institut du Développement de Ressources en Informatique Scientifique administered by the CNRS, for the calculation facilities. T. D. L. is grateful to the AUF for a doctoral fellowship. D. A. thanks the European Community for a post-doctoral fellowship (FSE).

Appendix A. Supplementary material

Supplementary data associated with this article can be found, in the online version, at doi:10.1016/j.jorganchem.2008.10.033.

References

- [1] W.W. Schoeller, *Top. Curr. Chem.* 229 (2003) 75.
- [2] (a) D. Gudat, *Coord. Chem. Rev.* 163 (1997) 71; (b) M. Sanchez, M.R. Mazières, L. Lamandé, R. Wolf, in: M. Regitz, O.J. Scherer (Eds.), *Multiple Bonds and Low Coordination in Phosphorus Chemistry*, Thieme, Stuttgart, 1990, p. 129; (c) A.H. Cowley, R.A. Kemp, *Chem. Rev.* 85 (1985) 367.
- [3] (a) J.J. Weigand, S.D. Riegel, N. Burford, A. Decken, *J. Am. Chem. Soc.* 129 (2007) 7969; (b) C.A. Dyker, N. Burford, M.D. Lumsden, A. Decken, *J. Am. Chem. Soc.* 128 (2006) 9632.
- [4] (a) J.M. Slattey, C. Fish, M. Green, T.N. Hooper, J.C. Jeffery, R.J. Kilby, J.M. Lynam, J.E. McGrady, D.A. Pantazis, C.A. Russell, C.E. Willans, *Chem. Eur. J.* 13 (2007) 6967; (b) N. Burford, C.A. Dyker, A. Decken, *Angew. Chem., Int. Ed.* 44 (2005) 2364; (c) N. Burford, D.E. Herbert, P. Ragogna, R. McDonald, M.J. Ferguson, *J. Am. Chem. Soc.* 126 (2004) 17067; (d) N. Burford, P. Ragogna, R. McDonald, M.J. Ferguson, *J. Am. Chem. Soc.* 125 (2003) 14404; (e) N. Burford, P. Ragogna, R. McDonald, M.J. Ferguson, *Chem. Commun.* (2003) 2066; (f) N. Burford, T.S. Cameron, P.J. Ragogna, E. Ocando-Mavarez, M. Gee, R. McDonald, R.E. Wasylshen, *J. Am. Chem. Soc.* 123 (2001) 7947; (g) N. Burford, T.S. Cameron, D.J. LeBlanc, P. Losier, S. Sereda, G. Wu, *Organometallics* 16 (1997) 4712; (h) D.C.R. Hockless, M.A. McDonald, M. Pabel, S.B. Wild, *J. Organomet. Chem.* 529 (1997) 189; (i) F. Sh. Shagvaleev, T.V. Zykova, R.L. Tarasova, T. Sh. Sitdikova, V.V. Moskva, *Zh. Obshch. Khim.* 60 (1990) 1775.
- [5] (a) N. Burford, P. Losier, A.D. Phillips, P.J. Ragogna, T.S. Cameron, *Inorg. Chem.* 42 (2003) 1087; (b) D. Gudat, A. Haghverdi, H. Hupfer, M. Nieger, *Chem. Eur. J.* 6 (2000) 3414; (c) V.A. Jones, S. Sriprang, M. Thornton-Pett, T.P. Kee, *J. Organomet. Chem.* 567 (1998) 199; (d) N. Burford, P. Losier, P.K. Bakshi, T.S. Cameron, *J. Chem. Soc., Chem. Commun.* (1996) 307; (e) G. Bouhadir, R.W. Reed, R. Reau, G. Bertrand, *Heteroat. Chem.* 32 (1995) 399; (f) T. Kaukorat, I. Neda, R. Schmutzler, *Coord. Chem. Rev.* 137 (1994) 53; (g) R.W. Reed, R. Reau, F. Dahan, G. Bertrand, *Angew. Chem., Int. Ed.* 32 (1993) 399; (h) C. Payrastré, Y. Madaule, J.G. Wolf, T.C. Kim, M.-R. Mazières, R. Wolf, M. Sanchez, *Heteroat. Chem.* 3 (1992) 157.
- [6] (a) S. Burck, D. Gudat, K. Nättinen, M. Nieger, M. Niemeyer, D. Schmid, *Eur. J. Inorg. Chem.* (2007) 5112; (b) S. Burck, D. Gudat, F. Lissner, K. Nättinen, M. Nieger, T. Scheid, *Z. Anorg. Allg. Chem.* 631 (2005) 2738; (c) C.J. Carmalt, V. Loleli, B.G. McBurnett, A.H. Cowley, *Chem. Commun.* (1997) 2095; (d) M.K. Denk, S. Gupta, R. Ramachandran, *Tetrahedron Lett.* 37 (1996) 9025.
- [7] (a) D. Gudat, *Eur. J. Inorg. Chem.* (1998) 1087; (b) R.J. Boyd, N. Burford, C.L.B. Macdonald, *Organometallics* 17 (1998) 4014.
- [8] T.D. Le, M.-C. Weyland, Y. El-Harouch, D. Arquier, L. Vendier, K. Miqueu, J.-M. Sotiropoulos, S. Bastin, A. Igau, *Eur. J. Inorg. Chem.* (2008) 2577.
- [9] (a) Similar behaviour has been previously reported: Z. Fei, R. Scopelliti, P.J. Dyson, *Eur. J. Inorg. Chem.* (2004) 530; (b) E.J. Nurminen, J.K. Mattinen, H. Lönnberg, *J. Chem. Soc., Perkin Trans. 2* (2001) 2159. and references therein.
- [10] T.D. Le, Ph.D. Thesis, Université de Toulouse, 2008.
- [11] C. Reichardt, *Solvents and Solvent Effects in Organic Chemistry*, 2nd ed., VCH, Weinheim, 1990.
- [12] H.J. Reich, WINDNMR-Pro: NMR Spectrum Calculation, Version 7.1.12.
- [13] CN bonds in organic formamidine derivatives have only partial double bond in character, see: (a) T.M. Krygowski, K. Wozniak, in: S. Patai, Z. Rappoport (Eds.), *The Chemistry of Amidines and Imidates*, John Wiley Sons Ltd., Chichester, 1991, p. 101; (b) A.G. Orpen, L. Brammer, F.H. Allen, O. Kennard, D.G. Watson, R. Taylor, in: H.-B. Bürgi, J.D. Dunitz (Eds.), *Structure Correlation*, Vol. 2, VCH, Weinheim, 1994, p. 770.
- [14] B.D. Ellis, P.J. Ragogna, C.L.B. Macdonald, *Inorg. Chem.* 43 (2004) 7857.
- [15] S.L. Buchwald, S.J. LaMaire, R.B. Nielsen, B.T. Watson, S.M. King, *Tetrahedron Lett.* 28 (1987) 3895.
- [16] M.J. Frisch, G.W. Trucks, H.B. Schlegel, G.E. Scuseria, M.A. Robb, J.R. Cheeseman, J.A. Montgomery, T. Vreven, Jr., K.N. Kudin, J.C. Burant, J.M. Millam, S.S. Iyengar, J. Tomasi, V. Barone, B. Mennucci, M. Cossi, G. Scalmani, N. Rega, G.A. Petersson, H. Nakatsuji, M. Hada, M. Ehara, K. Toyota, R. Fukuda, J. Hasegawa, M. Ishida, T. Nakajima, Y. Honda, O. Kitao, H. Nakai, M. X. Klene, X. Li, J.E. Knox, H.P. Hratchian, J.B. Cross, C. Adamo, J. Jaramillo, R. Gomperts, R.E. Stratmann, O. Yazyev, A.J. Austin, R. Cammi, C. Pomelli, J.W. Ochterski, P.Y. Ayala, K. Morokuma, G.A. Voth, P. Salvador, J.J. Dannenberg, V.G. Zakrzewski, S. Dapprich, A.D. Daniels, M.C. Strain, O. Farkas, D.K. Malick, A.D. Rabuck, K. Raghavachari, J.B. Foresman, J.V. Ortiz, Q. Cui, A.G. Baboul, S. Clifford, J. Cioslowski, B.B. Stefanov, G. Liu, A. Liashenko, P. Piskorz, I. Komaromi, R.L. Martin, D.J. Fox, T. Keith, M.A. Al-Laham, C.Y. Peng, A. Nanayakkara, M. Challacombe, P.M.W. Gill, B. Johnson, W. Chen, M.W. Wong, C. Gonzalez, J.A. Pople, *Gaussian 03*, Revision D-02, Gaussian, Inc., Pittsburgh, PA, 2003.
- [17] R.G. Parr, W. Yang, in: R. Breslow, J.B. Goodenough (Eds.), *Functional Theory of Atoms and Molecules*, Oxford University Press, New York, 1989.
- [18] P.C. Hariharan, J.A. Pople, *Theor. Chim. Acta* 28 (1973) 213.
- [19] (a) A.D. Becke, *Phys. Rev. A* 38 (1988) 3098; (b) A.D. Becke, *J. Chem. Phys.* 98 (1993) 5648; (c) C. Lee, W. Yang, R.G. Parr, *Phys. Rev. B* 37 (1988) 785.
- [20] (a) A.E. Reed, L.A. Curtiss, F. Weinhold, *Chem. Rev.* 88 (1988) 899; (b) J.P. Foster, F. Weinhold, *J. Am. Chem. Soc.* 102 (1980) 7211.
- [21] (a) Molekel 4.3, P. Flükiger, H.P. Lüthi, S. Portmann, J. Weber, Swiss Center for Scientific Computing, Manno, Switzerland, 2000–2002.; (b) S. Portmann, H.P. Lüthi, Molekel: An Interactive Molecular Graphics Tool, *Chimia* 54 (2000) 766.